Energy Conversion and Management 258 (2022) 115518

Contents lists available at ScienceDirect

Energy Conversion and Management

journal homepage: www.elsevier.com/locate/enconman

Combined cold supply system for ship application based on low GWP refrigerants - Thermo-economic and ecological analyses

Jan Wajs [a,*], Michal Mrozek [a], Elzbieta Fornalik-Wajs [b]

[a] Gdansk University of Technology, Faculty of Mechanical Engineering and Ship Technology, Institute of Energy, Narutowicza 11/12, 80-233 Gdansk, Poland
[b] AGH University of Science and Technology, Faculty of Energy and Fuels, Department of Fundamental Research in Energy Engineering, Mickiewicza 30, 30-059, Poland

ARTICLE INFO

Keywords:
Maritime refrigeration
Maritime air conditioning
Low GWP refrigerants
Carbon dioxide
Hydrofluoroolefins (HFOs)
Cold supply system efficiency

ABSTRACT

The withdrawal of popular high-GWP refrigerants will significantly affect maritime industry. Refrigeration and air conditioning systems currently used on ships are not ready to fulfil future limitations. Therefore, there is a need for system, which will operate with low-GWP refrigerants and at the same time will be efficient and reliable in difficult environmental conditions. This paper explains the concept of a cold supply system, in which refrigeration/freezing plant rejects heat not to a seawater but to a chilled water, produced by the air conditioning unit. Configuration of single stage compression with internal heat exchanger and HFO refrigerant was used in the air conditioning system, while in the refrigeration/freezing plant, two-stage compression trans-critical booster with R744 as refrigerant. Comparative thermodynamic analyses of presented concept with other configurations of thermodynamic cycles and refrigerants were performed. They were carried out in wide range of seawater temperature values and incorporated efficiency characteristics of compressors produced by a well-known manufacturers. Results confirmed ability of described system to improve energy efficiency in comparison with separated and currently used on ships cold supply systems, especially in hot climate. Economic and ecological analyses of proposed concept exhibited an additional benefit - positive environmental impact.

1. Introduction

It is widely recognized that the emission of carbon dioxide (CO_2) released into the atmosphere from human activities has reached worrying levels and has a significant impact on climate change. The 18 hottest years since the beginning of measurements have occurred in the last two decades. Global warming is transforming the environment by increasing the frequency and intensity of extreme weather events. Consequently, 195 countries have committed to reduce greenhouse gases (GHG) emission under the Paris Agreement. The long-term goal is to keep the average temperature increase on Earth significantly below 2 K compared to the preindustrial levels [1].

In 2005, the shipping sector accounted for 2.6% of global CO_2 emission [2], emitting approximately one billion tonnes of GHG annually in 2007–2015 [3]. The most recent estimates show that GHG emissions from total shipping have increased by 9.6%, from 977 million tonnes in 2012 to 1076 million tonnes in 2018. The share of shipping emissions in global anthropogenic GHG emissions changed from 2.76% in 2012 to 2.89% in 2018 [4]. According to the forecast of the International Maritime Organization (IMO), the growth in GHG emissions from ships by 2050 may reach the level of 20% to 250% compared to 2012, depending on the economic development scenario [3,5]. As other sectors of the economy reduce GHG emission, the shipping industry will account for an increasing share of global emission - without appropriate action, this share could reach 17% in 2050 [6]. There are several solutions to cut emissions and shift to low carbon shipping:

1) usage of energy-saving technologies that guarantee lower fuel consumption,
2) usage of renewable energy sources,
3) usage of fuels with a lower carbon content (e.g., biofuels) [7].

Although international shipping is excluded from the Paris Agreement, the IMO is developing its own strategy to reduce GHG emission from ships. The IMO Marine Environment Protection Committee (MEPC) has given extensive attention to the issue of controlling GHG emission and in 2011 adopted a resolution [8] introducing two instruments: the Energy Efficiency Design Index (EEDI) for newly built vessels, and the Ship Energy Efficiency Management Plan (SEEMP) for all ships. From January 1st of 2013, these regulations apply to all ships with a tonnage greater than 400 GT. The EEDI is the most important

* Corresponding author.
E-mail address: jan.wajs@pg.edu.pl (J. Wajs).

https://doi.org/10.1016/j.enconman.2022.115518
Received 31 December 2021; Received in revised form 2 March 2022; Accepted 17 March 2022

Nomenclature

h	specific enthalpy [kJ/kg]
m	total refrigerant charge [kg]
$m_{CO_2,eq}$	carbon dioxide equivalent total refrigerant charge [kg]
$\dot{m}$	mass flow rate [kg/s]
P	pressure [Pa]
P_C	compressor power [kW]
Q_0	cooling capacity [kW]
s	specific entropy [kJ/(kg·K)]
T	temperature [°C]

Greek symbols

α	coefficient
Δ	difference value,
δ	annual leaks of refrigerant [kg/year]
η_i	compressor isentropic efficiency [-]
π	compressor pressure ratio [-]

Abbreviations

AC	air conditioning
COP	cooling coefficient of performance
EEDI	energy efficiency design index
EU	European Union
GHG	greenhouse gases
GWP	global warming potential
HCFC	hydrochlorofluorocarbon refrigerant
HCFO	hydrochlorofluoroolefin refrigerant
HFC	hydrofluorocarbon refrigerant
HFO	hydrofluoroolefin refrigerant
HVACR	heating, ventilation, air conditioning and refrigeration
HGWP	high global warming potential
LGWP	low global warming potential
MSCB	multi-stage compression booster
R/F	refrigeration/freezing
SEEMP	ship energy efficiency management plan
SSC	single stage compression
SSCwEV	single stage compression with expansion valves
SSCwIHE	single stage compression with an internal heat exchanger

Subscripts

CON	conceptual system
critic	critical
CSS	cold supply system
cw,s	chilled water, supply
cw,r	chilled water, return
dis	discharge
HT	high temperature
I	first stage compressor
II	second stage compressor
IHE	internal heat exchanger
LT	low temperature
MT	medium temperature
opt	optimal
r	return
s	supply
SC	subcooling
SH	superheating
suc	suction
sw	seawater

technical measure to promote more energy-saving (and less polluting) technologies in newly constructed ships [8]. It indicates the minimum required level of energy efficiency for various vessel types and size segments, expressed in grammes of CO_2 emission per capacity mile (e.g., tonne mile). Units built in 1999–2009 were considered as the baseline and it was established that ships commissioned in 2020–2024 must be 20% more efficient, and those commissioned after 2024 30% more efficient than the baseline. On 13 April 2018, the MEPC accepted a resolution on the IMO's draft strategy to reduce GHG emission [9]. The vision of the IMO assumes a reduction of the emission by at least 50% until 2050 compared to 2008 levels, and their complete elimination after that date.

1.1. Refrigerants in maritime applications

Refrigerants currently used on ships have high Global Warming Potential (HGWP) values, a measure which indicates the effect of a given refrigerant on global warming when it leaks into the atmosphere. Trade in substances with the HGWP is regulated by numerous legal acts, such as the international Kigali Amendments introduced to the Montreal Protocol [10], or the Act on F-gases, which relates to the Member of the European Union. The European F-gas Regulation restricts the use of refrigerants with the GWP above 150 in some refrigeration equipment, gradually reduces the amount of F-gases to be introduced into the circulation, and strengthens the leakage checking, recovery and repair requirements for refrigeration equipment with HGWP refrigerants [11]. In addition, some specific national laws tax the purchase of HFC refrigerants, for example, in Denmark, Sweden, Germany, and Spain [12]. Although the use of HGWP refrigerants is not currently prohibited on ships, numerous international treaties and national regulations, imposing restrictions on this type of working fluid, justify the expectation of limiting the GWP of refrigerants in marine applications. Currently, some maritime registers only propose voluntary labelling for refrigeration systems with a low environmental impact, requiring a maximum GWP of the refrigerant of 1950 [13] or 2000 [14–16].

Restrictive environmental standards for refrigerants force both research and industry to use environmentally friendly working fluids when designing new cooling systems. Natural substances with low GWP (LGWP) include ammonia (R717, GWP = 0), CO_2 (R744, GWP = 1) or propane (R290, GWP = 3). In addition to environmental standards, an important aspect when selecting a refrigerant is also safety related requirements, i.e., toxicity and flammability/explosiveness, classified according to the American Society of Heating, Refrigerating and Air-Conditioning Engineers (ASHRAE) standards [17]. Considering safety, the best choice is CO_2, as a non-flammable and nontoxic (safety class A1) working fluid, recognized as the most promising refrigerant in the shipbuilding industry [18] in places, where ammonia cannot be used. Ammonia is a low flammable but toxic working fluid (safety class B2L). Furthermore, it has corrosive properties for copper, zinc, and their alloys, which forces the use of i.a. open compressors and steel piping. Propane, on the other hand, is non-toxic but explosive working fluid (safety class A3), which excludes it from being used in large cooling installations.

Synthetic refrigerants with the GWP below 150 include fluids belonging to the currently popular (but at the same time increasingly being withdrawn) hydrofluorocarbons (HFC) group, and to the new group of hydrofluoroolefin/hydrochloroolefin (HFO/HCFO) low-boiling fluids. HFC refrigerants include R152a (GWP = 138, safety class A2) and R161 (GWP = 4, safety class A3) [19]. Numerous regulations introduced in recent years will likely result in a gradual increase in their prices, which together with flammability make the HFC inadvisable. Among the fluids belonging to the HFO group, the following ones are most often

considered in refrigeration and air-conditioning equipment: R1234ze(E) (GWP = 1) and R1234yf (GWP = 4) [11]. Both fluids are assigned to the safety class A2L. Proposed HFO refrigerants have the same flammability as ammonia, which is successfully used on ships with appropriate safety control, but the new group of refrigerants does not have problems of toxicity and pungent odour that could, in the event of a leak, cause panic among the crew [18].

1.2. Maritime refrigeration/freezing system performance

Literature overview exhibits that the heating, ventilation, and air conditioning (HVAC) system is usually the second largest energy consumer on the ship (after the propulsion system) [20]. The paper [21] indicates that the air conditioning (AC) system on a frigate-type ship is responsible for over 40% of the total energy consumption. Traditionally, refrigeration/freezing (R/F) systems are based on the vapour compression systems [22]. GHG emission from this type of equipment can be divided into indirect and direct emissions. According to [23], more than 90% of the total emission from offshore cooling installations are indirect, i.e., due to the GHG generated by the production of electricity consumed by refrigeration equipment. This means that the key solution to reduce GHG emission from a cold supply system lies in its performance. In case of direct emission, refrigerant leaks from plants are accounting for about 2% of the total maritime GHG emission [18]. These leaks are a particular problem in marine refrigeration systems due to vibration and violent shocks caused by sea waves damaging pipelines. They are also responsible for lowering the efficiency of the system, and thus increasing indirect emission - the loss of 10% of the refrigerant from the installation results in a 20% higher energy consumption [18].

The increase in energy efficiency on the ship is also sought in the management of waste heat both for the purposes of electricity production [24,25] and cold supply with the use of absorption devices [26,20]. In turn, there is little research work focused on improving the efficiency of compressor refrigeration systems. One of the concepts considers combining the R/F and AC systems and was introduced in [18,23]. In paper [18], the idea of such a combination was only mentioned without any details referring to the proposed system (system configuration or kind of refrigerator used in AC system). The system presented in [23], called cascade, consisted of the R/F system based on the single stage compression cycles, separately considered for chilling and freezing purposes, and an AC plant formed by two-stage compression system with a flash tank. Applied refrigerants were R744 in freezing plant, R1234yf in AC plant and R717, R744, R1234yf and R1234ze(E) in chilling plant. Analyses were conducted for three operation points. The shortage of analysis discussing changes of the relation of AC power to R/F power and their influence on the introduced concept causes some doubts related to the possible application of this solution.

In the works [27,28], the authors considered a single-stage compression cycle with R134a refrigerant on board of a ship which operates on variable sea water temperature conditions. Coefficient of cooling performance (COP) values reached the level of 5.48 and 2.93, respectively, for the lower and upper limits of the considered sea water temperature range (18–40°C).

The paper [29] presents an analysis of the energy efficiency of a single-stage compression cycle operating in a cooling system on a cargo ship. The cycle was cooled with seawater at temperature value in the range of 18-40°C. Fifteen different refrigerants were analysed, including R134a, R407C, and R1234yf. The highest performance of the cooling system was reported for the R134a refrigerant.

2. Problem statement

Literature review exhibits a few problems which the cold supply sector in maritime industry will be soon facing, namely: reduction of GHG emission, withdrawal of currently used refrigerants, and required increase of cycle performance. There is no simple solution of these problems, since it will depend on many aspects: thermodynamic, ecological, and economical. One of the possible options, that can help to overcome the problems is the modification of existing systems and the application of new refrigerants.

This paper presents a proposal of an alternative cold supply system for ship application with ecological refrigerants. These studies mainly focused on cargo ships, which accounted for more than 68% of all merchant ships in the EU (at the end of 2006) [30]. The system consists of AC and R/F plants combined with each other and is more advanced than the cascade system presented in [18,23]. The cycle chosen for the analyses in AC plant is single stage compression with internal heat exchanger (SSCwIHE), while in R/F plant is the multistage compression booster cycle (MSCB). In this work, the compressor selection algorithm of well-known producer was used to determine the compressor internal efficiency in all analysed configurations of cycles and refrigerants. Energy performance of the proposed cold supply system was compared to a system with separated AC and R/F plants and in addition, with the currently used on ships one. Analyses were conducted for the most popular in maritime industry HGWP refrigerants (R404A, R407C and R134a) and LGWP refrigerants, including R744. All energy analyses were performed for a wide range of refrigerants condensation temperature values. The paper summarizes the advantages and disadvantages of the considered systems, taking into account technical, ecological, and economic aspects. Presented assessment of proposed system demonstrated its potential, especially for ships operating in hot climate. It should be emphasized that it fulfils all near future environmental requirements.

3. Reference system

The simplicity, reliability, and price have a dominant influence on the selection of the cold supply system for ship applications. Therefore, they are usually realizing the most basic cycles, despite more effective and at the same time more complex thermodynamic cycles with evaporation at one temperature [31] and at multiple temperature values [32]. According to [30], AC systems used on ships are mostly indirect ones based on the single stage compression (SSC) thermodynamic cycle. The central unit cools the water, which in turn receives heat from air-conditioned rooms on board. In the case of a R/F, the direct systems are used with evaporators located in the refrigeration and freezing chambers and a condensing unit located in the engine room. The most commonly used thermodynamic cycle is already mentioned SSC cycle, in which the evaporation temperature values in the refrigeration chambers are controlled by separate expansion valves (SSCwEV). Described AC and R/F plants (shown in Fig. 1) are the parts of the currently used ship's cold supply system, which is taken as a reference one and marked as Ref (HGWP).

Seawater [29] or fresh water from a central cooling system [33] are used as the coolant for condensers of AC and R/F plants. Utilization of seawater causes corrosion and fouling of the heat exchangers. The use of water from the central cooling system allows to avoid seawater disadvantages and provides stable operating conditions of the cold supply system due to a constant temperature of the coolant during the cruise. However, it may result in a reduction of the cold supply system efficiency due to the required higher refrigerants condensation temperature value. This is because the fresh water temperature in the central cooling system is kept constant at the level of 36°C [33]. This temperature is higher than the sea water temperature, which may vary from 0°C to over 35°C, depending on the area where the ship is voyaging [34].

At the end of 2006, 75% of all refrigerants used on European ships was refrigerant R22 (GWP = 1,700), belonging to HCFC group [35]. This refrigerant has been banned since 2001 because its leakage from the installation destroys the stratospheric ozone layer. The remaining 25% accounted for refrigerants from the HFC group: R134a (GWP = 1,430) in AC systems and R404A (GWP = 3,922) in R/F systems [30]. In the shipbuilding industry of the Nordic countries in 2013–2016, the

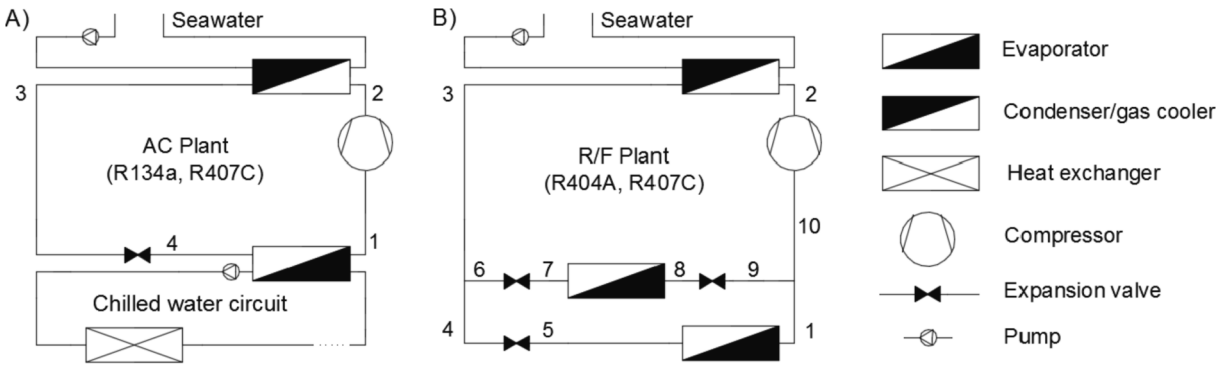

Fig. 1. Schematic diagram of the ship's cold supply system – **Ref(HGWP):** A) AC Plant - single stage compression (SSC), B) R/F Plant - single stage compression with expansion valves (SSCwEV).

dominant working fluids in AC systems were R134a, R407C, and R404A. On the other hand, in R/F systems R404A and R407C (GWP = 1,774) were used [18]. In accordance with the literature, in the presented analyses, following refrigerants will be considered in Ref(HGWP): AC plant – R134a, R407C and R/F plant – R404A, R407C (see Fig. 1).

4. Proposed concept

The schematic diagram of the proposed system is presented in Fig. 2.

The proposed solution assumes the possibility of using chilled water generated in the air conditioning plant as a coolant for the condenser/gas cooler of the R/F plant. It allows to lower the condensing temperature in the cycle, increasing its efficiency. During nonoperation periods of the AC system, seawater acts as the primary coolant for the condenser/gas cooler of the R/F.

In the article, the authors assumed that the demand for cold from the air conditioning system will occur when the seawater temperature is equal to 18°C or is higher. It means that the chilled water production process starts at seawater temperature of 18°C.

The circulation of chilled water as an intermediate medium is forced by the pump. Water, transported from the evaporator in the appropriate amount, controlled by a three-way valve, is directed to the condenser of the R/F plant. Then it goes to the T-pipe, where it is mixed with the stream of chilled water returning from air-conditioned rooms and directed back to evaporator of AC unit.

The presented concept requires an additional modification of the R/F system in the form of two three-way valves and a heat exchanger acting as a condenser. The proposed heat exchanger is a brazed plate heat exchanger, compact and relatively cheap. Two three-way valves in nodal points 5 and 6 (in Fig. 2) are responsible for controlling the flow of the refrigerant and selecting the heat exchanger in which its vapour will condense/cool. A heat exchanger cooled with chilled water will be used above seawater temperature value equal to 22°C (following the analyses conducted in Section 5), while below this temperature value heat exchanger will be cooled with seawater. Increase of the cooling capacity of the AC system is also required due to the additional heat that must be removed from the R/F condenser.

Considering the thermodynamic cycle for the AC, the single-stage compression cycle with the internal heat exchanger (SSCwIHE) while for the R/F, the multistage compression booster cycle (MSCB) were chosen. These cycles are characterised by an increase in the complexity of the system compared to the reference one (currently used in the shipbuilding industry), especially in the case of R/Fs, however, they are also characterised by higher efficiency, and thus by lower energy consumption.

According to [36] trans-critical multistage compression booster cycle has become a well-established configuration over the past 10 years. The trans-critical state of R744 in a cycle results in reduced thermodynamic losses and improved convective heat transfer. The considered cycle has become standard market solution for new installation especially in cold climate regions where it outperforms the conventional synthetic refrigerant-based system. Therefore, refrigeration companies related to the shipbuilding industry are working on adapting such a system to marine conditions and low cooling capacities.

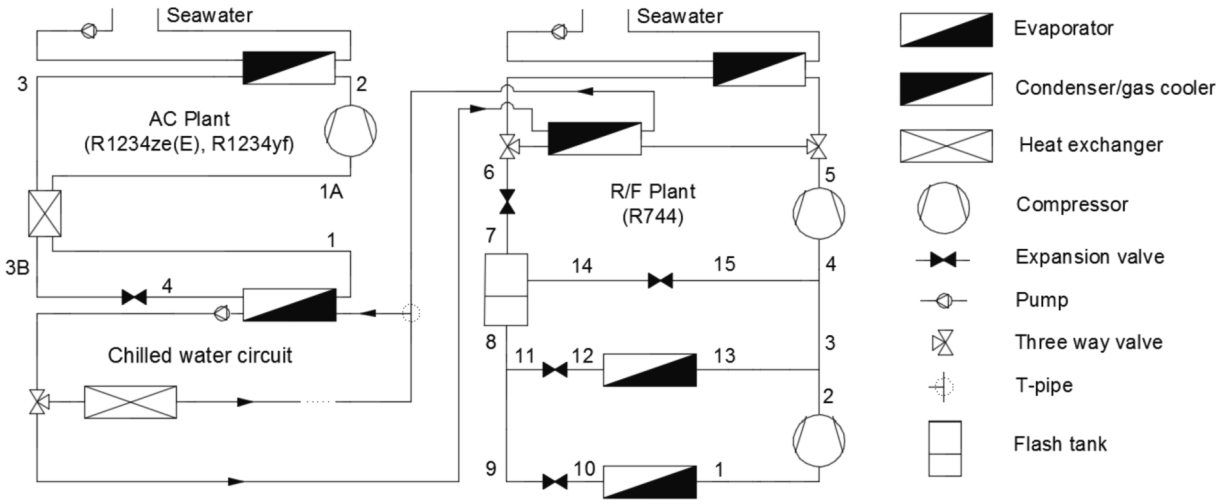

Fig. 2. Schematic diagram of the combined cold supply system on a ship – **CONCEPT**: AC Plant – single stage compression with internal heat exchanger (SSCwIHE); R/F Plant – multi-stage compression booster (MSCB).

In the proposed AC system, two synthetic refrigerants from the HFO group were considered, namely, R1234yf and R1234ze(E) while in R/F system R744.

The combined AC and R/F plants (Fig. 2) with **CONCEPT** designation to facilitate the tracking of the analysis results will be compared to:

(1) reference system presented in Fig. 1, with HGWP refrigerants (R134a, R407C, and R404A) – **Ref(HGWP)**,
(2) systems with the same thermodynamic cycles and refrigerants as in the proposed concept, but separated. Schematic diagram of the system is presented in Fig. 3 – **Sep(LGWP).**

5. Thermodynamic analysis

5.1. Assumptions

To compare proposed concept with the solutions reported in literature [23,27–29] the assumption of constant cooling capacity was performed. In accordance with [30] it was assumed that the usable AC system capacity in each of the presented systems is 150 kW, while the total capacity of the R/F system is 10 kW. The cooling capacity of the freezing chamber was assumed to be 3 kW and the cooling capacity of the refrigeration chamber was 7 kW.

The heat from cold supply systems is transferred from the condenser/gas cooler to the outboard supplied seawater. The condenser/gas cooler is cooled by the seawater, which temperature variation was assumed to be in the range $T_{sw} = 0 - 40$°C. The work of seawater pumping was not included in the analysis. Particular attention was paid to the coolant temperature of 36°C, which is maintained in the central cooling network on ships [33].

The condenser/gas cooler was treated as a counter-current heat exchanger. The temperature difference between seawater at the inlet of the heat exchanger and the refrigerant at the outlet (ΔT_{HT}) was set at 5 K. Since no subcooling in the condenser was assumed, the temperature difference represented the difference between the seawater temperature and the refrigerant condensation temperature.

The exception to this assumption was for R744, which due to its properties in the supercritical region (i.e. above $T_{critic} = 30.987$°C reduced the temperature difference [18,37]. The assumed minimum temperature difference values in the R744 condenser/gas cooler in the near-critical region of this refrigerant are shown in Table 1. For coolant temperature values below 26°C, the difference (ΔT_{HT}) was 5 K, while for temperature values above 28°C it was 3 K.

The temperature of the refrigerant at the outlet of the condenser/gas cooler was thus calculated according to the following equation:

Table 1
Minimum temperature difference in the R744 condenser/gas cooler near the critical point of R744.

Temperature of condenser/gas cooler coolant	T_{sw}[°C]	25	26	27	28	29
Temperature of R744 at the outlet of the condenser/gas cooler	T_{HT}[°C]	30	31	31	31	32
Temperature difference	ΔT_{HT}[K]	5	5	4	3	3

$$T_{HT} = T_{sw} + \Delta T_{HT} \quad (1)$$

When the temperature (T_{HT}) exceeded refrigerant critical point temperature, pressure in the gas cooler had to be adjusted to achieve the maximum efficiency of the cycle. In other words, in a trans–critical cycle, for a constant R744 gas exit temperature, there is an optimum value of gas pressure ($P_{gc,opt}$) that maximises the COP of the system operating at the same evaporating temperature [37,38]. The optimal pressure is identified by the authors manually by changing the α [-] coefficient for a set temperature to find the highest COP:

$$P_{gc,opt} = \alpha \cdot P_{critic} \quad (2)$$

where, P_{critic} was critical pressure of R744.

The AC is operating as an indirect system: a central unit known as a chiller cools the water (preparing chilled water), which is pumped to heat exchangers located in rooms requiring cooling. The intermediate system is a closed-circuit system with a designed temperature of chilled water at the supply to the AC system equal to $T_{cw,s} = 7$°C, and at the return $T_{cw,r} = 12$°C. The evaporation temperature in the AC system was assumed to be $T_{AC} = 2$°C, and the degree of vapor superheating at the outlet of the evaporator $\Delta T_{SH} = 5$ K. The pump operation in the chilled water circuit was omitted in these considerations. Analyses of AC systems were carried out for seawater as the condenser coolant considered in the temperature range of 18–40°C.

The refrigeration and freezing of provisions were realized with the use of a cycle with direct evaporation of the working fluid. The refrigerant evaporation temperature in the freezing chamber was assumed at the level of $T_{LT} = -29$°C, and in the refrigerating chamber $T_{MT} = -4$°C. In both cases, the degree of refrigerant vapor superheating in the evaporators was assumed to be: $\Delta T_{SH} = 5$ K. Analyses of R/F plants were carried out in the range of condenser coolant temperature values between 0°C and 40°C.

Thermodynamic models of cold supply cycles were based on the conservation of mass and energy equations. The following assumptions were done in the model:

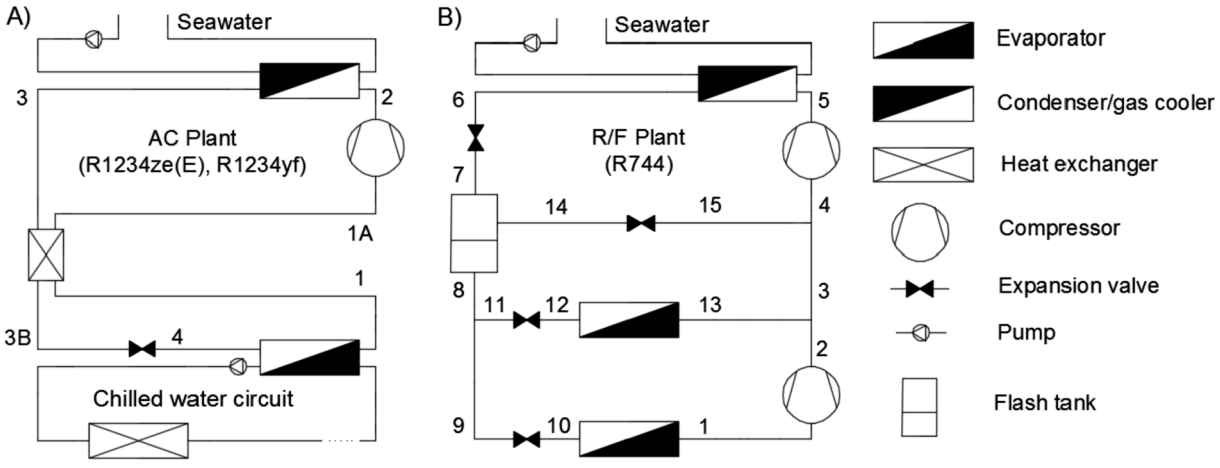

Fig. 3. Schematic diagram of the ship's cold supply system - **Sep(LGWP):** A) AC Plant - single stage compression with internal heat exchanger (SSCwIHE); B) R/F Plant - multistage compression booster (MSCB).

- the system operates in steady state,
- pressure drops in pipelines and heat exchangers are neglected,
- heat losses/gains from the environment in system components (pipeline, valves, etc.) are neglected,
- the specific enthalpy values at the inlet and outlet of the expansion valves are equal,
- there is no subcooling of the refrigerant in the condenser,
- compressors operate with internal (isentropic) efficiency determined on the basis of the type of cycle and the selected refrigerant, and calculated using the compressor selection program created by the Bitzer company [39],
- the cooling of the compressor electric motor with refrigerant vapour is omitted (it means that the increase in the specific enthalpy of the refrigerant at the suction side of the compressor is not taken into account),
- in the cycle with the internal heat exchanger, the subcooling of the refrigerant in the IHE (ΔT_{SC}) is selected manually [40]. The difference between the temperature of the saturated liquid refrigerant entering the heat exchanger and the temperature of the superheated vapor sucked in by the compressor from the heat exchanger (ΔT_{IHE}) was set to 5 K. This relation is presented in Eq. (3), where the temperature subscripts refer to Fig. 3A. This kind of assumption allows maximising the subcooling for every operating point of the cycle, thus maximising efficiency [40,41].

$$\Delta T_{IHE} = 5\ K = T_3 - T_{1A} \tag{3}$$

Properties of working fluids were determined using the Refprop 9.1 software [42].

5.2. Thermodynamic cycles

Equations used to determine the caloric and thermal parameters of the refrigerants at the nodal points of individual cycles are summarized in Table 2. The symbols denoted by subscripts correspond to the relevant figures indicated in the table headings.

5.3. Performance of the system

A measure of the cooling efficiency of counter-clockwise thermodynamic cycles is the coefficient of performance (COP) defined as the ratio of the total cooling capacity of a cycle (Q_0) to the total power of the compressors operating in this cycle (P_c). It is described as:

$$COP = \frac{Q_0}{P_C} \tag{4}$$

Equations showing the calculation method of the total cooling capacity and compressor power in individual cycles are summarized in Table 2.

The coefficient of performance of the entire cold supply system (COP_{CSS}) was calculated by dividing the total, useful cooling capacity of the system (AC and R/F plants) by the total power of the compressors:

$$COP_{CSS} = \frac{Q_{0,AC} + Q_{0,R/F}}{P_{C,AC} + P_{C,R/F}} \tag{5}$$

In the proposed concept, lowering the condensation temperature in the multi-stage compressor booster cycle by using chilled water as the condenser coolant reduces the power of the compressors in the R/F plant resulting in a higher coefficient of performance.

However, this is not an actual increase in the R/F plant efficiency as it does not take into account the compressor power increase in the AC plant. This is induced by higher cooling capacity of the AC unit working in combination with R/F plant ($Q_{0,AC,CON}$), in accordance with the following equation:

$$Q_{0,AC,CON} = Q_{0,AC} + Q_{HT,R/F} \tag{6}$$

The compressor power increase in an AC plant in the concept system ($\Delta P_{C,AC,CON}$) was determined using the relation:

$$\Delta P_{C,AC,CON} = P_{C,AC,CON} - P_{C,AC} \tag{7}$$

where $P_{C,AC,CON}$ is power of the AC compressor operating in the concept system (Fig. 3) calculated with the following equation:

$$P_{C,AC,CON} = \frac{Q_{0,AC,CON}}{COP_{AC}} \tag{8}$$

Taking into account above considerations, the actual cooling coefficient of performance of the R/F plant in concept system ($COP_{R/F,CON}$) is given as:

$$COP_{R/F,CON} = \frac{Q_{0,R/F}}{P_{C,R/F} + \Delta P_{C,AC,CON}} \tag{9}$$

The cooling coefficient of performance of the entire, combined cold supply system ($COP_{CSS,CON}$) was calculated using the relation:

$$COP_{CSS,CON} = \frac{Q_{0,AC} + Q_{0,R/F}}{P_{C,AC,CON} + P_{C,R/F}} \tag{10}$$

5.4. Compression process

During the analyzes, the use of screw (in the AC plants, except for R744 refrigerant) and reciprocating compressors (in the R/F plants and the AC plant with R744 refrigerant) was assumed. The compressors were selected for the plants using a Bitzer software [38]. As input parameters, the program uses: type of working fluid, its evaporation and condensation temperature, degree of vapor superheating in the evaporator (useful superheat) and at the compressor inlet. The result of the program is, among others, the refrigerant temperature at the compressor outlet ($T_{dis,B}$). The authors of this paper decided to determine the isentropic (internal) efficiency of the compressors to reproduce the operating parameters at the end of the compression process during further analyses, based on the data published by a well-known compressor supplier.

To determine the isentropic efficiency of the compressor, in the first step, parameters at the suction pipe of the compressor were calculated for every cycle. For this purpose, the equations presented in Table 2 were used.

The third degree polynomial approximations of the compressor efficiency characteristics depending on the compressor pressure ratio have been listed in Table 3. They were used in modelling of thermodynamic cycles to find parameters of the refrigerant at the end of the compression process.

In the case of systems operating in the subcritical cycle, the compressor discharge pressure (condensation/gas cooling pressure) was determined taking into account the function described by Eq. (11). For R744 in the supercritical cycle it was read from the Bitzer compressor selection program:

$$P_{dis} = f(T_{HT}, x = 1) \tag{11}$$

The temperature and specific enthalpy at the end of isentropic compression ($s_{suc} = s_{dis,s}$) were calculated using Eqs. (12) and (13):

$$h_{dis,s} = f(P_{dis}, s_{suc}) \tag{12}$$

$$T_{dis,s} = f(P_{dis}, h_{dis,s}) \tag{13}$$

Taking into account temperature in the discharge pipe indicated by the compressor selection program ($T_{dis,B}$), the specific enthalpy of the refrigerant at the end of the compression process with the compressor chosen by Bitzer software was obtained in accordance with Eq. (14):

$$h_{dis,B} = f(T_{dis,B}, P_{dis}) \tag{14}$$

The isentropic efficiency of the compression process was determined using the formula:

Table 2
Equations used for analyses of individual thermodynamic cycles.

SSC (Fig. 1A)	SSCwIHE (Fig. 3A)	SSCwEV (Fig. 1B)	MSCB (Fig. 3B)
COMPRESSION:	COMPRESSION:	COMPRESSION:	COMPRESSION:
$P_1 = f(T_{AC}, x = 1)$	$P_{1A} = P_1$	$P_{10} = f(T_{LT}, x = 1)$	$P_1 = f(T_{LT}, x = 1)$
$T_1 = T_{AC} + \Delta T_{SH}$	$h_{1A} = h_1 + (h_3 - h_{3B})$	$h_{10} = \frac{h_9 \cdot \dot{m}_9 + h_1 \cdot \dot{m}_1}{\dot{m}_9 + \dot{m}_1}$	$T_1 = T_{LT} + \Delta T_{SH}$
$h_1 = f(P_1, T_1)$	$s_{1A} = f(P_{1A}, h_{1A})$	$s_{10} = f(P_{10}, h_{10})$	$h_1 = f(P_1, T_1)$
$s_1 = f(P_1, h_1)$	$T_{1A} = f(P_{1A}, h_{1A})$	$T_{10} = f(P_{10}, h_{10})$	$s_1 = f(P_1, h_1)$
$P_{2s} = P_2 = P_3$	$P_{2s} = P_2 = P_3 = P_{3B}$	$P_{2s} = P_2 = P_3$	$P_{2s} = P_2$
$h_{2s} = f(P_{2s}, s_1)$	$h_{2s} = f(P_{2s}, s_{1A})$	$h_{2s} = f(P_{2s}, s_{10})$	$h_{2s} = f(P_{2s}, s_1)$
$h_2 = \frac{h_{2s} - h_1 + h_{2s} \cdot \eta_i}{\eta_i}$	$h_2 = \frac{h_{2s} - h_{1A} + h_{2s} \cdot \eta_i}{\eta_i}$	$h_2 = \frac{h_{2s} - h_{10} + h_{2s} \cdot \eta_i}{\eta_i}$	$h_2 = \frac{h_{2s} - h_1 + h_{2s} \cdot \eta_i}{\eta_i}$
$s_2 = f(P_2, h_2)$	$s_2 = f(P_2, h_2)$	$s_2 = f(P_2, h_2)$	$s_2 = f(P_2, h_2)$
$T_2 = f(P_2, h_2)$	$T_2 = f(P_2, h_2)$	$T_2 = f(P_2, h_2)$	$T_2 = f(P_2, h_2)$
$P_C = \dot{m}_1 \cdot (h_2 - h_1)$	$P_C = \dot{m}_1 \cdot (h_2 - h_{1A})$	$P_C = \dot{m}_{10} \cdot (h_2 - h_{10})$	$P_4 = P_3 = P_2$
			$P_4 = P_{13} = f(T_{MT}, x = 1)$
			$h_4 = \frac{h_{15} \cdot \dot{m}_{15} + h_3 \cdot \dot{m}_3}{\dot{m}_{15} + \dot{m}_3}$
			$s_4 = f(P_4, h_4)$
			$T_4 = f(P_4, h_4)$
			$P_{5s} = P_5 = P_6$
			$h_{5s} = f(P_{5s}, s_4)$
			$h_5 = \frac{h_{5s} - h_4 + h_{5s} \cdot \eta_i}{\eta_i}$
			$s_5 = f(P_5, h_5)$
			$T_5 = f(P_5, h_5)$
			$P_{C,I} = \dot{m}_{10} \cdot (h_2 - h_1)$
			$P_{C,II} = \dot{m}_4 \cdot (h_5 - h_4)$
			$P_C = P_{C,I} + P_{C,II}$
CONDENSATION:	CONDENSATION:	CONDENSATION:	CONDENSATION:
$T_{HT} = T_3$	$T_{HT} = T_3$	$T_{HT} = T_3$	$T_{HT} = T_6$
$P_3 = f(T_3, x = 0)$	$T_3 < T_{critic}$	$T_3 < T_{critic}$	$T_6 < T_{critic}$
$h_3 = f(P_3, x = 0)$	$P_3 < P_{critic}$	$P_3 < P_{critic}$	$P_6 < P_{critic}$
$s_3 = f(P_3, h_3)$	$P_3 = f(T_3, x = 0)$	$P_3 = f(T_3, x = 0)$	$P_6 = f(T_6, x = 0)$
$Q_{HT} = \dot{m}_2 \cdot (h_3 - h_2)$	$h_3 = f(P_3, x = 0) s_3 = f(P_3, h_3)$	$h_3 = f(P_3, x = 0)$	$h_6 = f(P_6, x = 0)$
	GAS COOLING:	$s_3 = f(P_3, h_3)$	$s_6 = f(P_6, h_6)$
	$T_3 > T_{critic}$	GAS COOLING:	GAS COOLING:
	$P_3 > P_{critic}$	$T_3 > T_{critic}$	$T_6 > T_{critic}$
	$P_3 = \alpha \cdot P_{critic}$	$P_3 > P_{critic}$	$P_6 > P_{critic}$
	$h_3 = f(P_3, T_3)$	$P_3 = \alpha \cdot P_{critic}$	$P_6 = \alpha \cdot P_{critic}$
	$s_3 = f(P_3, h_3)$	$h_3 = f(P_3, T_3)$	$h_6 = f(P_6, T_6)$
	$Q_{HT} = \dot{m}_2 \cdot (h_3 - h_2)$	$s_3 = f(P_3, h_3)$	$s_6 = f(P_6, h_6)$
		$Q_{HT} = \dot{m}_2 \cdot (h_3 - h_2)$	$Q_{HT} = \dot{m}_5 \cdot (h_6 - h_5)$
		T-PIPES:	T-PIPES:
		$T_3 = T_4 = T_6$	$T_8 = T_9 = T_{11}$
		$P_3 = P_4 = P_6$	$P_8 = P_9 = P_{11}$
		$h_3 = h_4 = h_6$	$h_8 = h_9 = h_{11}$
		$s_3 = s_4 = s_6$	$s_8 = s_9 = s_{11}$
			$P_3 = P_2$
			$h_3 = \frac{h_{13} \cdot \dot{m}_{13} + h_2 \cdot \dot{m}_2}{\dot{m}_{13} + \dot{m}_2}$
			$s_3 = f(P_3, h_3)$
			$T_3 = f(P_3, h_3)$
EXPANSION:	EXPANSION:	EXPANSION:	EXPANSION:
$h_3 = h_4$	$h_{3B} = h_4$	$h_4 = h_5$	$h_6 = h_7$
		$P_5 = P_1$	$P_7 = \sqrt[2]{P_2 \cdot P_6}$
		$T_5 = f(P_5, h_5)$	$T_7 = f(P_7, h_7)$
		$s_5 = f(P_5, h_5)$	$s_7 = f(P_7, h_7)$
		$x_5 = f(P_5, h_5)$	$x_7 = f(P_7, h_7)$
		$h_6 = h_7$	$h_{10} = h_9$
		$P_7 = P_8$	$P_{10} = P_1$
		$T_7 = f(P_7, h_7)$	$T_{10} = f(P_{10}, h_{10})$
		$s_7 = f(P_7, h_7)$	$s_{10} = f(P_{10}, h_{10})$
		$x_7 = f(P_7, h_7)$	$x_{10} = f(P_{10}, h_{10})$
		$h_8 = h_9$	$h_{12} = h_{11}$
		$P_9 = P_1$	$P_{12} = P_{13}$
		$T_9 = f(P_1, h_9)$	$T_{12} = f(P_{12}, h_{12})$
		$s_9 = f(P_1, h_9)$	$s_{12} = f(P_{12}, h_{12})$
			$h_{15} = h_{14}$
			$P_{15} = P_4$
			$T_{15} = f(P_{15}, h_{15})$
			$s_{15} = f(P_{15}, h_{15})$

(*continued on next page*)

Table 2 (*continued*)

SSC (Fig. 1A)	SSCwIHE (Fig. 3A)	SSCwEV (Fig. 1B)	MSCB (Fig. 3B)
EVAPORATION: $Q_0 = \dot{m}_4 \cdot (h_1 - h_4)$	EVAPORATION: $P_1 = f(T_{AC}, x = 1)$ $T_1 = T_{AC} + \Delta T_{SH}$ $h_1 = f(P_1, T_1)$ $s_1 = f(P_1, h_1)$ $Q_0 = \dot{m}_4 \cdot (h_1 - h_4)$	EVAPORATION: $P_1 = f(T_{LT}, x = 1)$ $T_1 = T_{LT} + \Delta T_{SH}$ $h_1 = f(P_1, T_1)$ $s_1 = f(P_1, h_1)$ $P_8 = f(T_{MT}, x = 1)$ $T_8 = T_{MT} + \Delta T_{SH}$ $h_8 = f(P_8, T_8)$ $s_8 = f(P_8, h_8)$ $Q_{0,LT} = \dot{m}_5 \cdot (h_1 - h_5)$ $Q_{0,MT} = \dot{m}_7 \cdot (h_8 - h_7)$ $Q_0 = Q_{0,LT} + Q_{0,MT}$	EVAPORATION: $P_{13} = f(T_{MT}, x = 1)$ $T_{13} = T_{MT} + \Delta T_{SH}$ $h_{13} = f(P_{13}, T_{13})$ $s_8 = f(P_{13}, h_{13})$ $Q_{0,LT} = \dot{m}_{10} \cdot (h_1 - h_{10})$ $Q_{0,MT} = \dot{m}_{12} \cdot (h_{13} - h_{12})$ $Q_0 = Q_{0,LT} + Q_{0,MT}$
	INTERNAL HEAT EXHANGER: $T_{3B} = T_3 - \Delta T_{SC}$ $P_{3B} = P_3$ $h_{3B} = f(T_{3B}, P_{3B})$ $s_{3B} = f(P_{3B}, h_{3B})$ $h_3 - h_{3B} = h_{1A} - h_1$		FLASH TANK: $P_7 = P_8 = P_{14}$ $x_8 = 0$ $T_8 = f(P_8, x_8)$ $h_8 = f(P_8, x_8)$ $s_8 = f(P_8, h_8)$ $x_{14} = 1$ $T_{14} = f(P_{14}, x_{14})$ $h_{14} = f(P_{14}, x_{14})$ $s_{14} = f(P_{14}, x_{14})$
MASS BALANCE: $\dot{m}_1 = \frac{Q_0}{(h_1 - h_4)}$ $\dot{m}_1 = \dot{m}_2 = \dot{m}_3 = \dot{m}_4$	MASS BALANCE: $\dot{m}_1 = \frac{Q_0}{(h_1 - h_4)}$ $\dot{m}_1 = \dot{m}_2 = \dot{m}_3 = \dot{m}_4$ $\dot{m}_1 = \dot{m}_{1A}$ $\dot{m}_3 = \dot{m}_{3B}$	MASS BALANCE: $\dot{m}_1 = \frac{Q_{0,LT}}{(h_1 - h_5)}$ $\dot{m}_1 = \dot{m}_5 = \dot{m}_4$ $\dot{m}_7 = \frac{Q_{0,MT}}{(h_8 - h_7)}$ $\dot{m}_7 = \dot{m}_6 = \dot{m}_8 = \dot{m}_9$ $\dot{m}_{10} = \dot{m}_1 + \dot{m}_9$ $\dot{m}_{10} = \dot{m}_2 = \dot{m}_3$	MASS BALANCE: $\dot{m}_1 = \frac{Q_{0,LT}}{(h_1 - h_{10})}$ $\dot{m}_1 = \dot{m}_2 = \dot{m}_9 = \dot{m}_{10}$ $\dot{m}_{13} = \frac{Q_{0,MT}}{(h_{13} - h_{12})}$ $\dot{m}_{13} = \dot{m}_{12} = \dot{m}_{11}$ $\dot{m}_8 = \dot{m}_9 + \dot{m}_{11}$ $\dot{m}_3 = \dot{m}_{13} + \dot{m}_2$ $\dot{m}_4 = \dot{m}_{15} + \dot{m}_3$ $\dot{m}_4 = \dot{m}_5 = \dot{m}_6 = \dot{m}_7$ $\dot{m}_7 = \dot{m}_8 + \dot{m}_{14}$ $\dot{m}_{14} = \dot{m}_{15}$

Table 3
Approximation functions of the compressor efficiency characteristics depending on the compressor pressure ratio for the analysed configuration of the cycles and refrigerants. The symbol R^2 represents coefficient of determination.

Description	Function	R^2
R134a (SSC), AC	$\eta_i = 0.027646 \cdot \pi^3 - 0.316770 \cdot \pi^2 + 1.185851 \cdot \pi - 0.762605$	0.9998
R407C (SSC), AC	$\eta_i = 0.024729 \cdot \pi^3 - 0.288233 \cdot \pi^2 + 1.067591 \cdot \pi - 0.595972$	0.9980
R744 (SSC), AC	$\eta_i = 0.078618 \cdot \pi^3 - 0.630916 \cdot \pi^2 + 1.664090 \cdot \pi - 0.747131$	0.9949
R1234yf (SSC), AC	$\eta_i = 0.022702 \cdot \pi^3 - 0.263584 \cdot \pi^2 + 1.016007 \cdot \pi - 0.557920$	0.9994
R1234ze(E) (SSC), AC	$\eta_i = 0.024262 \cdot \pi^3 - 0.276709 \cdot \pi^2 + 1.034950 \cdot \pi - 0.584986$	0.9990
R404A (SSCwEV), R/F	$\eta_i = -0.000037 \cdot \pi^3 - 0.000222 \cdot \pi^2 + 0.006186 \cdot \pi + 0.644283$	0.9888
R744 (MSCB-I), R/F	$\eta_i = 0.61$	–
R744 (MSCB-II), R/F	$\eta_i = 0.027491 \cdot \pi^3 - 0.232774 \cdot \pi^2 + 0.654877 \cdot \pi - 0.042826$	0.9197

$$\eta_c = \frac{(h_{dis,s} - h_{suc})}{(h_{dis,B} - h_{suc})} \tag{15}$$

The above procedure was used to find the characteristics of the internal efficiency of compressors in the cycles depending on the compression pressure ratio. Fig. 4 presents the characteristics of compressors used in AC plants and Fig. 5 of compressors used in R/F plants.

Two configurations of R/F plant, namely: R744 (SSCwEV) and R407C (SSCwEV) were excluded from the analysis, because the lowest evaporation temperature equal to −25°C was found for R407C refrigerant and the highest condensation temperature equal to 15°C was found for the single-stage compression cycle with R744. They do not fulfil the limits of the compressors and assumptions made by the authors.

Designation R744 (MSCB-II) in Fig. 5 refers to the second compressor stage in a multistage booster compression system. Rapid change in the efficiency of the compressor at 2.5–3 compression pressure ratio is caused by the transition of R744 from the subcritical region to the transcritical region. The first stage compressor in the multistage cycle has a constant isentropic efficiency ($\eta_{i,I} = 0.61$).

6. Performance results and their discussion

6.1. Air conditioning plant

Results of calculations for individual configurations in the AC plant are presented in Fig. 6.

The COP of the system with R134a refrigerant in tested temperature range is, on average, 18.32% higher than the COP achieved by the cycle with R407C. At condenser coolant temperature equal to 40°C cycle with the R134a has 27.05% higher COP than cycle with R407C. Therefore, a single-stage compression cycle with R134a refrigerant in the AC plant represented the installations currently operating on the ship board.

The average COP in indicated condenser/gas cooler temperature range is calculated as the arithmetic mean of the coefficients of performance, as shown in the equation below:

$$COP_{AV} = \frac{COP(T_1) + COP(T_1 + 1) + \cdots + COP(T_n)}{n} \tag{16}$$

where:

$COP(T_1)$ – coefficient of performance with condenser/gas cooler temperature at the beginning of the indicated range (T_1),

$COP(T_n)$ – coefficient of performance with condenser/gas cooler temperature at the end of the indicated range (T_n).

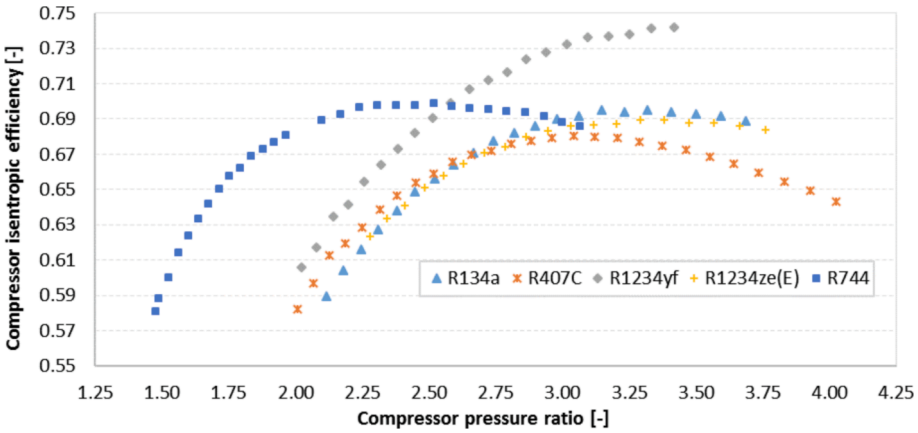

Fig. 4. Internal (isentropic) efficiency of compressors used in AC plants depending on the compressor pressure ratio.

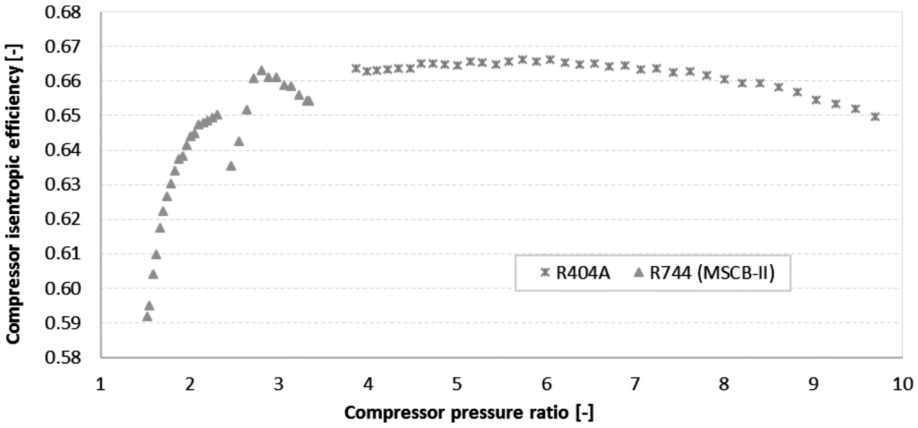

Fig. 5. Internal (isentropic) efficiency of compressors used in R/F plant depending on the compressor pressure ratio.

Among the new eco-friendly refrigerants working in the single-stage compression cycle in tested temperature range the most effective system is R1234yf. At condenser coolant temperature values below 28°C system with R1234ze(E) is slightly more efficient, but it changes with temperature increase. At condenser coolant temperature equal to 40°C cycle with the R1234yf has 2.97% higher COP than cycle with R1234ze(E).

Natural refrigerant R744 has much lower performance compared to cycles that use synthetic refrigerants. The flattening of the COP distribution at coolant temperature values between 26°C and 28°C occurs due to the transition of the R744 cycle to a supercritical mode of operation, and the reduction of the temperature difference between the coolant of the condenser/gas cooler and the refrigerant at the heat exchanger outlet from 5 K to 3 K.

For a single-stage compression cycle with an internal heat exchanger, the R1234yf is most effective refrigerant. At condenser coolant temperature equal to 40°C cycle with the R1234yf has 5.88% higher COP than cycle with R1234ze(E), and 101.66% higher COP than cycle with R744. The COP of the system with R1234yf refrigerant in tested temperature range is, on average, 61.61% higher than the COP achieved by the cycle with R744.

The use of an internal regeneration heat exchanger allowed to obtain an increase in COP (average value in the whole analysed temperature range) by 4.44% for the cycle with R1234yf, 2.95% for the cycle with R1234ze(E) and 1.09% for the cycle with R744.

Alternative AC system with SSCwIHE cycle and the R1234yf shows higher COP in the entire analysed temperature range of the condenser coolant compared to the currently used single-stage cycle with the R134a refrigerant. The improvement in COP at condenser coolant temperature of 40°C is equal to 11.54%. Average COP in the entire analysed condenser coolant temperature range is 4.96% higher in case of alternative AC system.

For further analyses, a single-stage compression system with an internal heat exchanger filled with LGWP refrigerant R1234yf was selected. This configuration, assuming the temperature of the condenser coolant corresponding to the central cooling system (36°C), is characterised by a compressor power of 34.86 kW. For comparison, the power of compressors in a single-stage compression cycle with the refrigerants currently used is 47.51 kW (+36.30%) for R407C and 37.82 kW (+8.49%) for R134a. Natural refrigerant R744 in a single-stage cycle with an internal heat exchanger requires compressors at the same coolant temperature with a power of 66.72 kW (+91.40%).

6.2. *Refrigeration and freezing plant*

Results of the energy analysis of individual cycle configurations in the R/F plant in relation to the temperature of the condenser/gas cooler coolant are presented in Fig. 7. Use of the multi-stage compressor booster cycle with R744 refrigerant results in a higher COP compared to the currently used on cargo ship R/F plant configuration. System with natural refrigerant has 73.15% higher COP at a temperature of the condensers coolant equal to 0°C. At a temperature of 18°C, the COP is 27.46% higher. Average COP of MSCB cycle with R744 refrigerant is 49% higher in the condenser coolant temperature range of 0–18°C than COP of currently used R/F system with R404A refrigerant and 33.56% higher in the entire analysed condenser coolant temperature range. However, as the coolant temperature increases, the COP of the R744 cycle drops, meeting the values of many simpler cycles with synthetic refrigerant at a condenser coolant temperature of 40°C. Lowering the

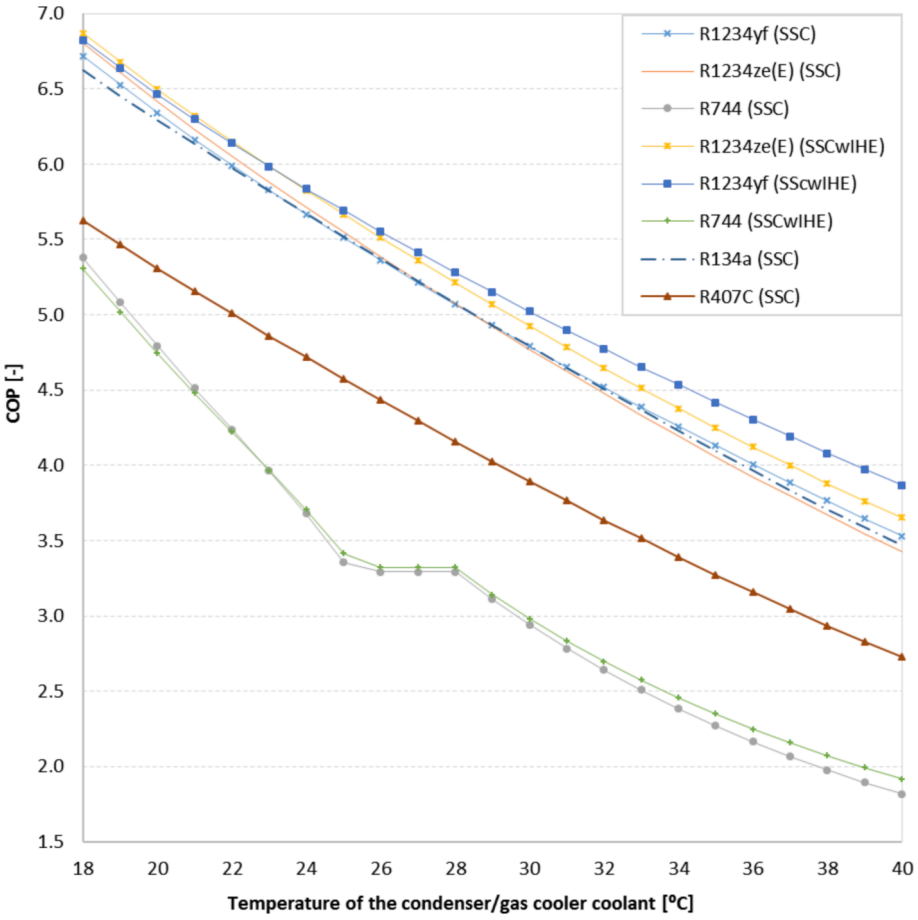

Fig. 6. Cooling coefficient of performance of the AC system for various configurations of the refrigerant/ thermodynamic cycle, depending on the temperature of the condenser/gas cooler coolant.

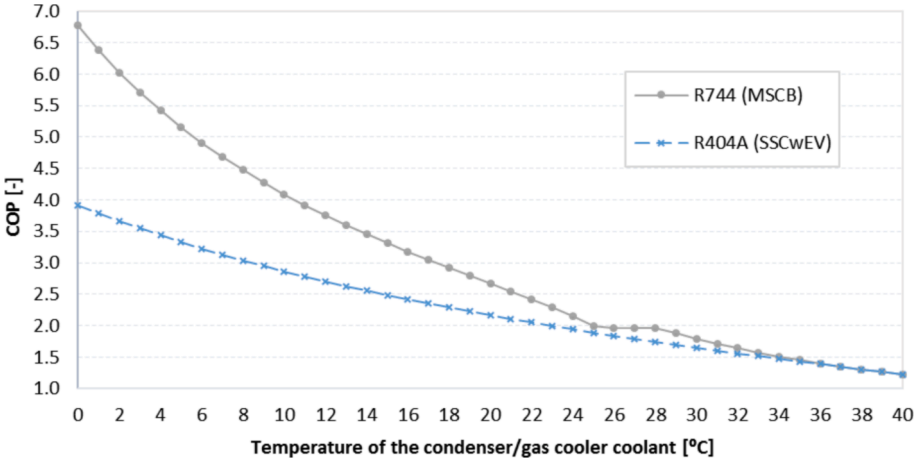

Fig. 7. Cooling coefficient of performance of the R/F for various configurations of the refrigerant/thermodynamic cycle, depending on the temperature of the condenser/gas cooler coolant.

temperature of the coolant from 40°C to 0°C results in a 3.19-fold increase in COP of the HFC refrigerant, while in the case of the natural working fluid - as much as 5.52 times.

By using water at a temperature of 36°C from the central cooling system to cool the condenser/gas cooler of the R744 system, COP = 1.4 is obtained, while in the case of the currently used system COP is equal to 1.39. Performance is almost the same, but the R744 system is much more complex and expensive. With the current gentle approach to carbon dioxide emissions from ships, this solution would not be welcomed by investors. However, an extension of the European emissions trading scheme to the shipbuilding industry [43] is considered, and it will increase interest in cleaner and more technologically advanced systems.

6.3. Concept system

Fig. 8 presents the reduction of power of compressors in the R/F system and the increase in the power of the AC system compressor after combining these systems in accordance with the proposed concept. Calculation results are plotted as a function of the temperature of the condenser/gas cooler coolant. The power reduction due to the higher R/F plant COP exceeds the power increase of the AC plant resulted from higher cooling capacity above the condenser coolant temperature of 22°C. Considering this result, it was concluded that chilled water should be directed to the condenser of the R/F unit at the sea water temperature above 22°C.

The power reduction of the R/F compressor in the proposed system is constantly rising with temperature. Assuming the use of an indirect central cooling circuit on ship, in which the water used to cool the condensers is kept at a constant temperature of 36°C, the reduction of compressors power in the R/F plant in the proposed conceptual system is equal to 2.19 kW. For comparison, power of the compressor at the same condenser coolant temperature in the reference R404a (SSCwEV) configuration is equal to 7.19 kW and 7.14 kW in R744 (MSCB) configuration working without combining with AC plant. This leads to 30.45% reduction of compressor power in comparison to the currently used R/F plant and to 30.67% in comparison to R744 (MSCB) configuration which works separately. As the condenser coolant temperature rises to 40°C, these values increase to 35.17% (2.86 kW) for both configurations.

Fig. 9 presents the COP of individual configurations of the refrigerant/thermodynamic cycle used for refrigeration and freezing provisions depending on the temperature of the condenser/gas cooler coolant. The condenser/ gas cooler coolant temperature is limited to 18–40°C as this is the area that shows the differences between the reference system and the proposed system. In the temperature range of 0–22°C, the R/F cycle with R744 presents the same COP values as in a separate installation shown in Fig. 9 (R744 (MSCB)). Average COP of the proposed system in the temperature range of condenser/gas cooler coolant equal to 22–40°C is higher by about 33.93% in comparison to the reference R404A (SSCwEV) configuration and 25.06% in comparison to R744 (MSCB) configuration.

6.4. Comparison of various ship types

The proposed concept has also been verified for a various power ratio of the AC to R/F systems on other ships.

Based on [30], a comparison of different cold supply systems depending on the merchant ship type was prepared, presenting their types, power, and average amount of refrigerant in these systems (Table 4). Presented data apply to AC plants (indirect and direct) with R134a and R/F plants with R404A.

Data included in Table 4, were used to estimate the proportion between the amount of refrigerant and cooling capacity for various types of plants:

(1) 1 kg of refrigerant corresponds to 2 kW of cooling capacity in AC plant with indirect evaporation;
(2) 1 kg of refrigerant corresponds to 1 kW of cooling capacity in AC and R/F systems, when the evaporation of the medium is carried out directly.

Different types of ship have different R/F to AC power ratios. The power ratio influences the increase in the cooling coefficient of performance provided by the proposed concept. The analysis shows a percentage increase in the cooling coefficient of performance (ΔCOP) of the combined system in comparison to the system working in a separated configuration at temperature of the condenser/gas cooler coolant equal to 36°C. Calculation results are presented in Table 5.

$$\Delta COP[\%] = \frac{\Delta COP}{COP_{CSS}} \cdot 100\% \tag{17}$$

$$\Delta COP[-] = COP_{CSS,CON} - COP_{CSS} \tag{18}$$

The total efficiency improvement of the combined cold supply system depends on the ratio of the cooling capacity of the R/F to AC plant. A higher ratio $\left(Q_{0,R/F}/Q_{0,AC}\right)$ provides a higher performance gain for the entire combined cooling system.

Despite the smaller percentage increase in system coefficient of performance for a cruise ship, the absolute values of the fuel and carbon dioxide emission savings could be higher. The reason for this is significantly greater R/F and AC power values.

7. Ecological analysis

As part of the ecological analysis, the direct emission of the refrigerant from the cooling installation to the atmosphere was considered, as well as the indirect emission resulting from the production of electricity supplied to the cooling installation. Direct emission calculations were based on the data referring to the refrigerant amount in the AC and R/F plants on a cargo ship, indicated in accordance with conclusions from the data presented in Table 4 and they are listed in Table 6.

As the analysed AC plant is an indirect system, where 1 kg of refrigerant results in 2 kW cooling capacity [30], and the amount of refrigerant in the 150 kW plant is 75 kg. According to the proposed concept, the cooling capacity of the AC plant will increase to 162.14 kW. This results in a refrigerant charge of 81.07 kg. In the R/F plant (direct system), 1 kg of refrigerant results in 1 kW of cooling capacity [30], and

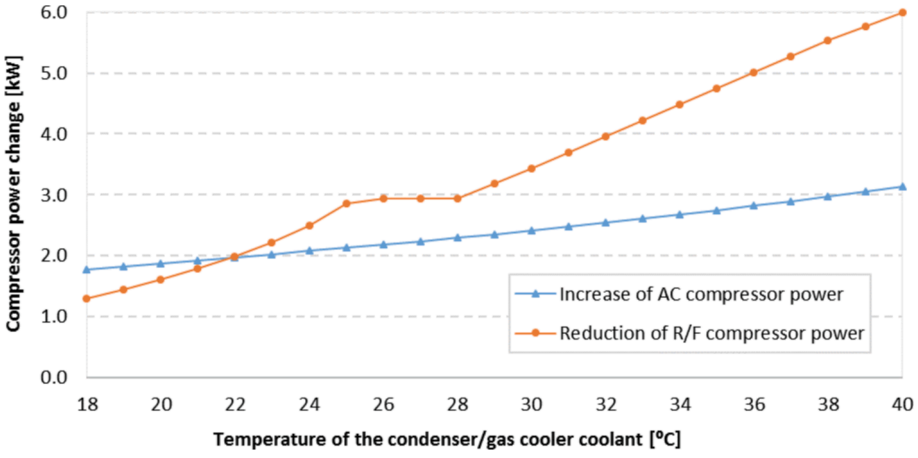

Fig. 8. Change in power of compressors when using the proposed concept depends on the temperature of the condenser/gas cooler coolant.

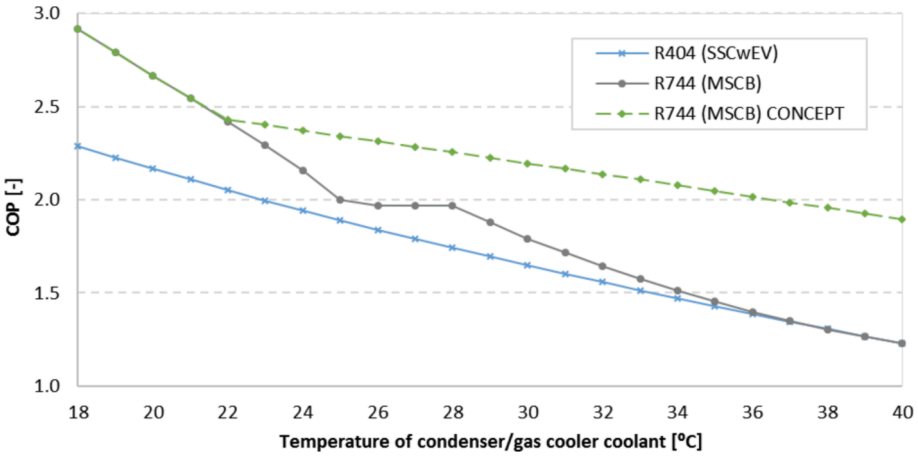

Fig. 9. Cooling coefficient of performance of R/F system in various configurations refrigerant/thermodynamic cycle, depending on the temperature of the condenser/gas cooler coolant.

Table 4
Average cooling capacity, type of the system, and amount of refrigerants in AC and R/F plants depending on the merchant ship type.

Ship type	R/F Refrigerant charge [kg]	System type	$Q_{0,R/F}$[kW]	AC Refrigerant charge [kg]	System type	$Q_{0,AC}$[kW]
Passanger ships	20	direct	20	500	indirect	1,000
Cruise ships	400	direct	400	6,000	Indirect	12,000
Cargo ships	10	direct	10	150	direct	150

Table 5
The effect of the proposed concept, taking into account the ship type. Result presented for temperature of the condenser/gas cooler coolant equal to 36°C.

Ship type	$Q_{0,R/F}$[kW]	$Q_{0,AC}$[kW]	$\frac{Q_{0,R/F}}{Q_{0,AC}}$[−]	ΔCOP [%]
Passanger ship	20	1,000	0.020	+1.81
Cruise ship	400	12,000	0.033	+2.93
Cargo ship	10	150	0.067	+5.49

so in the analysed 10 kW plant the amount of refrigerant is 10 kg in each case. Assumed charge values of refrigerants are having only pictorial character and do not take into account the properties of particular refrigerants and the differences in systems construction.

According to [30], the annual refrigerant loss in AC with an indirect system was assumed to be 20% of the total amount of refrigerant in the installation. The R/F system is a direct system, for which the annual refrigerant loss was assumed at the level of 40% of the total amount of refrigerant in the installation [30]. Taking the above into account, the annual leaks of refrigerants (δ) are, respectively:

- $\delta_{AC,HGWP} = \delta_{AC,LGWP} = 15$ kg,
- $\delta_{AC,CON} = 16.21$ kg,
- $\delta_{R/F} = 4$ kg.

Loss of individual refrigerants was converted into CO_2 equivalent according to Eq. (19):

$$m_{CO_2,eq} = \delta \cdot GWP \quad (19)$$

where:

$m_{CO_2,eq}$ – annual CO_2 emission equivalent caused by the loss of refrigerant from the installation [kg/year],

GWP – GWP of the refrigerant [-].

In the case of R/Fs, the CO_2 equivalent emissions are 4 kg/year when using R744 and 15,688 kg/year when using R404A refrigerant. Therefore, the use of a natural refrigerant allows to avoid direct emissions with the carbon dioxide equivalent of 15,684 kg per year.

In the case of AC plant operating not in combination with R/F ($Q_{0,AC}$ = 150 kW), annual CO_2 emission equivalent are, respectively:

- 26,610 kg for R407C,
- 21,450 kg for R134a,
- 60 kg for R1234yf,
- 15 kg for R1234ze(E),
- 15 kg for R744.

The AC plant operating in combination with the R/F plant ($Q_{0,AC}$ = 162.14 kW), filled with the R1234yf refrigerant, emits directly 64.86 kg of CO_2 equivalent per year.

The Sep(LGWP) system with the R1234yf refrigerant in the AC plant and the R744 refrigerant in the R/F plant avoids direct emissions of 42,234 kg CO_2 equivalent per year compared to the Ref(HGWP) system with the R407C refrigerant in the AC plant and the R404A refrigerant in the R/F plant.

When estimating indirect emission caused by generating electricity on board, data from the publication [44] were used. The authors indicated fuel consumption (marine gas oil (MGO)) per unit of electricity, amounting to 213 g_{MGO}/kWh. The emission of CO_2 resulting from fuel

Table 6
Estimated exemplary cooling capacity for proposed system operating on cargo ships.

Ship type	R/F plant Refrigerant charge [kg]	System type	$Q_{0,R/F}$[kW]	AC plant Refrigerant charge [kg]	System type	$Q_{0,AC}$[kW]
Cargo ships	10	direct	10	81.07	indirect	162.14

combustion, which is equal to 3.206 t_{CO_2}/t_{MGO} was also provided in the paper. Combining the above, the CO_2 emission per unit of electricity generated on the ship from MGO fuel was obtained: 682.88 g_{CO_2}/kWh.

In [44] data referring to the shipping time was also provided in following form: an annual shipping time of a container ship, 6,481 h, of which 3,987 h is navigation in water with temperature values above 20°C. The analysis of indirect emission assumed the use of a central cooling system with a constant temperature of 36°C on the ship. Under such conditions, the cold supply system will run 2,494 h in split mode, and for 3,987 h it will be possible to use chilled water as the condenser coolant for R/F plant (concept system). Combined system was compared with the reference one and with the system utilising cycles from the presented concept working separately throughout the year. Results are summarized in Table 7.

Summarizing the direct and indirect emissions and taking into account the amount of fuel used to produce electricity for the cold supply system on a cargo ship, the following conclusions were drawn:

- a separated system with LGWP refrigerants saves 2.564 tonnes of fuel per year (6.10%) and reduces the total CO_2 emission by 45.294 t (−26.35%) compared to the current cooling system,
- the proposed system saves 4.420 tonnes of fuel per year (10.52%) and reduces the total CO_2 emissions by 51.241 t (−29.81%) compared to the currently used cooling system,
- the proposed system saves 1.857 tonnes of fuel per year (4.70%) and reduces the total CO_2 emissions by 5.948 t (−4.70%) compared to cooling system with same thermodynamic cycles and refrigerants but working separately.

Additional analyses were conducted to investigate the effect of water temperature in the central cooling system on the total annual reduction of CO_2 emissions. The results of the analyses are shown in Fig. 10. Above the water temperature of 22°C, reduction of total CO_2 emissions resulting from the implementation of the concept system is constantly growing. Assuming that the water temperature in the central cooling system is equal to 40°C, the total annual reduction of CO_2 emissions for the concept system is over 57 tonnes.

Fig. 11 shows the annual reduction in total CO_2 emissions (direct and indirect) with different cold supply systems and variable annual navigation time with seawater temperatures above 20°C.

In the literature related to the shipbuilding industry, the ecological analyses carried out for the fleet of ships (e.g., 15 ships, according to the paper [29]), can be found. Taking into account the demand for the cooling capacity of the air-conditioned rooms of 150 kW and the total cooling capacity of the R/F system of 10 kW for a cargo ship, with a fleet of 15 ships and an assumed 10-year lifetime of cooling installations, the following results are obtained:

(1) a separated system with LGWP refrigerants saves 385 t of fuel and reduces the total CO_2 emission by 6,794 t compared to the cold supply system currently used;
(2) the proposed system saves 663 t of fuel and reduces the total CO_2 emission by 7,686 t compared to the cold supply system currently used.

Taking into account the current Global Average Bunker Price of Marine Gas Oil (USD 651.50/t_{MGO}) [45] and the environmental fee (EUR 55/t_{CO2} = USD 66.7/t_{CO2}) [46,47], this calculation gives the following amounts:

(1) USD 703,714 for 15 ships during 10 years,
(2) USD 944,660 for 15 ships during 10 years.

This means that the proposed concept allows to save an additional USD 240,946 (34.24%) over system with the same cycles and refrigerants but working separately. For one ship and one year, that is USD 1,606. It is worth noting that this result was obtained assuming that the combined system operates for 61.51% of the time the ship spends at sea. Fig. 12 shows the change in additional reduction of total costs by using the proposed concept instead of a system with the same cycles and refrigerants but working separately as a function of the annual navigation time with seawater temperatures above 20°C. Assuming the fleet will only operate in waters above 20°C (6,481 h instead of 3,987 h), the proposed concept allows for additional annual savings of USD 391,966 (43.26%). For one ship and one year, that is USD 2,611.

Taking into account dynamic increase in EU ETS price, calculated savings for different carbon tax prices are presented in Fig. 13. The data shows savings for one vessel over a period of one year from modernization of the reference system to the one proposed in this article (combined one). Price of EUR 125 per tonne of CO_2 is assumed based on Sweden Carbon Tax price [48]. Price of EUR 25 per tonne of CO_2 is to give perspective. The price of the EU ETS rose by 100% from EUR 25 to EUR 50 in just over seven months, and over 20 times in last 5 years [49]. The presented data show that with the current EU ETS price of over EUR 60 per tonne and in case of EU ETS in ship industry the cost savings resulting from the reduction of CO_2 emissions are greater than the savings from the reduction of fuel consumption.

The authors are aware of the simplification of adopting a fixed fuel price, but the presented data are intended to show the situation that will take place after the shipbuilding industry is included in the emissions trading system. Moreover, when analyzing the change in the MGO fuel price over the last 3 years [44], it can be seen that the fuel price adopted in the analyzes is 18.71% lower than the highest price in the described period (USD 801.5/t_{MGO}). Such a trend will indicate an even greater pressure from the shipping industry to reduce CO_2 emissions.

Table 7
Results of the ecological analyses of the different cold supply systems.

Cold supply system	Electrical energy [MWh]	Fuel [t]	Indirect CO_2 emission [t]	Direct CO_2 emission [t]	TOTAL CO_2 emission [t]
Ref (HGWP)	197.317	42.029	134.744	37.138	171.882
Sep (LGWP)	185.281	39.465	126.524	0.064	126.588
Difference	−12.037	−2.564	−8.220	−37.074	−45.294
	−6.10%	−6.10%	−6.10%	−99.83%	−26.35%
Ref (HGWP)	197.317	42.029	134.744	37.138	171.882
CONCEPT	176.564	37.608	120.572	0.069	120.641
Difference	−20.753	−4.420	−14.172	−37.069	−51.241
	−10.52%	−10.52%	−10.52%	−99.81%	−29.81%
Sep (LGWP)	185.281	39.465	126.524	0.064	126.588
CONCEPT	176.564	37.608	120.572	0.069	120.641
Difference	−8.717	−1.857	−5.952	0.005	−5.948
	−4.70%	−4.70%	−4.70%	7.59%	−4.70%

8. Summary

The adaptation of cold supply systems on ships to new global demands, such as increasing the efficiency of devices and reducing the impact of human activity on the environment, is required. In the literature, the only proposal of increasing the cold supply system efficiency through improving the efficiency of compressor refrigeration systems was found in [18,23]. Since the analysis has not included all necessary data and details (e.g., definition of conditions suitable for system application), there were some doubts referring to the presented solution. Therefore, the authors proposed a more advanced combined system, in which the R/F plant based on the multistage compression booster, while the AC unit, slightly more complicated than those currently used and filled with new synthetic refrigerants from the HFO group. This approach provides a higher cooling coefficient of performance for the cold supply system. As a result, electricity consumption

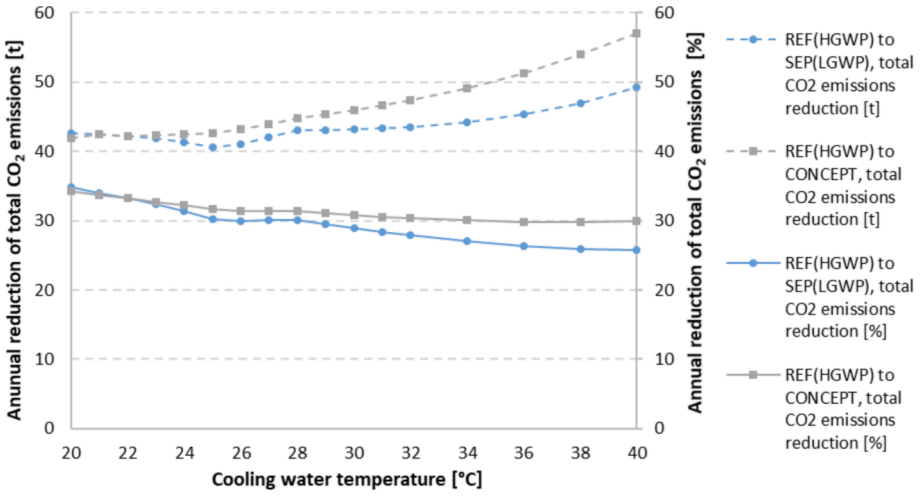

Fig. 10. Annual reduction in total CO_2 emissions per ship with different cold supply system and variable water temperature in central cooling system.

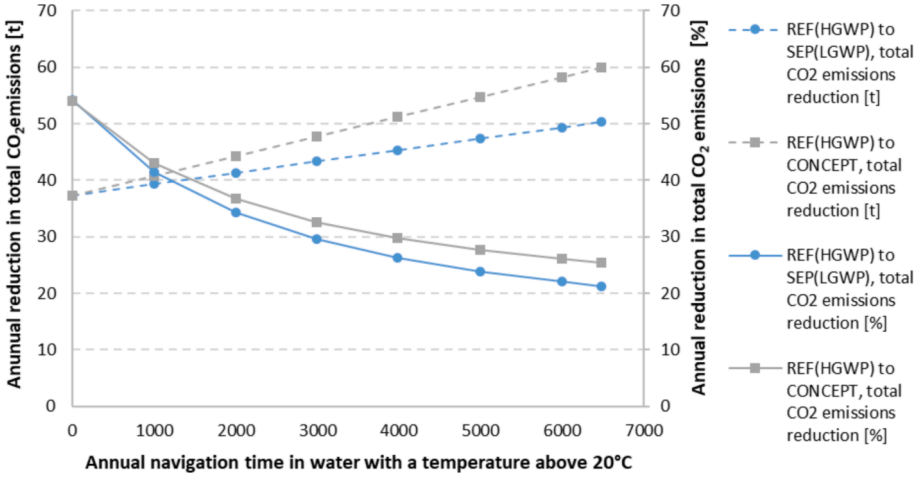

Fig. 11. Annual reduction in total CO_2 emissions per ship with different cold supply system and variable annual navigation time in water temperature above 20°C.

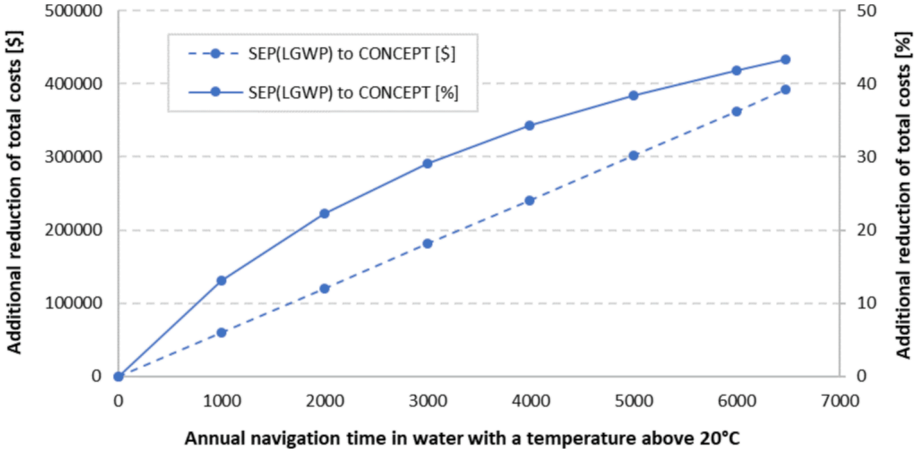

Fig. 12. Additional reduction of total costs with a fleet of 15 ships and an assumed 10-year installation lifetime by using CONCEPT instead of SEP(LGWP) configuration, depending on annual navigation time in water temperature above 20°C.

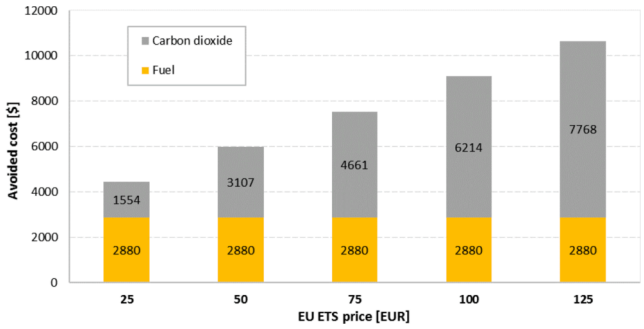

Fig. 13. Annual savings per ship resulting from replacing the reference system with the proposed combined one depending on EU ETS prices. Assumed fuel price: USD 651.50/t_{MGO}.

and thus the air pollution are reduced, since the ship's electricity is generated from fossil fuels. The use of new working fluids with a much smaller impact on global warming than those currently used significantly reduces the negative influence on the environment in the event of a possible leakage of the fluid.

In general, the systems utilizing R744 as the refrigerant for maintaining provision within appropriate parameters achieve higher cooling coefficients of performance at low temperature values of the condenser coolant, but their performance drastically decreases at high coolant temperature values. The proposed concept allows to improve the efficiency of the R/F system with a natural refrigerant at high temperatures of the condenser coolant. This significantly improves its attractiveness compared to the currently used systems with synthetic refrigerants from the HFC group. Additional deficiencies and benefits of the proposed system indicated by the presented analysis are:

- small increase in system performance at low seawater temperature values,
- strong relationship between the increase in cooling coefficient of performance and growth in cost of the cold supply system with high value of $Q_{0,R/F}/Q_{0,AC}$ coefficient,
+ great reduction in GHG emission,
+ savings in fuel and environmental costs,
+ usage of ecological refrigerant.

These lists clearly indicate that the proposed system is a potential option in the ship industry. The limitations in the temperature range suitable for the proposed system were precisely defined. The possible cooling coefficient of performance improvement depending on the condenser coolant temperature is indicated, as well as the possible energy savings for various ratios of R/F and AC power values.

There is one more issue the authors would like to mention here, namely, ecological analysis and its possible, but hard to obtain improvement. To conduct a more detailed analysis referring to the refrigerant leakage to the atmosphere, a precise determination of refrigerant amount in the cold supply system is required. For this purpose, it is necessary to know the technical details of the cold supply system, designed for a particular ship, for example, the pipelines length, parameters of heat exchangers and compressors, etc. In addition, the characteristics of the cooling demand as a function of the ambient temperature as well as the power and energy consumption data of the chilled water pumps are necessary. This data would help to determine the volume occupied by the refrigerant and its mass and to be close to the real systems. Unfortunately, it very often is not available, therefore it was emphasized that the improvement could be hard to obtain.

Considering all the disadvantages and advantages, it can be said that the proposed system seems to be the most suitable for cargo and cruise ships operating mainly in the hot climate. Additionally, it meets all new environmental requirements.

Funding

The results presented in this paper were obtained from a research work co-financed by the National Centre of Research and Development in the framework of Contract POIR.01.02.00-00-0009/18 – INNOship Programme. Participation of E. Fornalik-Wajs was supported by Ministry of Education and Science (Grant AGH No. 16.16.210.476).

CRediT authorship contribution statement

Jan Wajs: Conceptualization, Methodology, Validation, Formal analysis, Writing – review & editing, Investigation, Supervision, Project administration, Funding acquisition. **Michal Mrozek:** Conceptualization, Methodology, Validation, Formal analysis, Investigation, Data curation, Visualization, Writing – original draft, Writing – review & editing. **Elzbieta Fornalik-Wajs:** Validation, Formal analysis, Writing – original draft, Writing – review & editing, Supervision.

Declaration of Competing Interest

The authors declare that they have no known competing financial interests or personal relationships that could have appeared to influence the work reported in this paper.

References

[1] UNFCCC, 2015. Adoption of the Paris Agreement, https://unfccc.int/resource/docs/5/cop21/eng/l09r01.pdf [access online 16.07.2020].
[2] Olmer N., Comer B., Roy B., Mao X., Rutherford D.: Greenhouse gas emissions from global shipping, 2013–2015; The international council on clean transportation (ICCT); October 2017.
[3] International Maritime Organization. Third IMO GHG study 2014, executive summary and final report. Suffolk, UK: Printed by micropress Printers; 2015.
[4] International Maritime Organization. Fourth IMO GHG study 2020. Executive summary: Published by the International Maritime Organization, London, UK; 2021.
[5] CE Delft Committed to the Environment (2017) Update of maritime greenhouse gas emission projections. Report prepared for BIMCO, publication code: 17.7I69.67; https://www.cedelft.eu/en/publications/2056/update-of-maritime-greenhouse-gas-emission-projections [access online 28.07.2020].
[6] Cames, M., Graichen, J., Siemons, A., Cook, V., 2015. Emission reduction targets for international aviation and shipping, viewed 06 December 2015, ⟨http://www.europarl.europa.eu/RegData/etudes/STUD/2015/569964/IPOL_STU(2015) 569964_EN.pdf⟩.
[7] Rehmatullaa N, Calleyab J, Smith T. The implementation of technical energy efficiency and CO_2 emission reduction measures in shipping. Ocean Eng 2017;139: 184–97. https://doi.org/10.1016/j.oceaneng.2017.04.029.
[8] The Marine Environment Protection Committee; Resolution MEPC.203(62): Amendments to the annex of the protocol of 1997 to amend the international convention for the prevention of pollution from ships, 1973, as modified by the protocol of 1978 relating thereto (Inclusion of regulations on energy efficiency for ships in MARPOL Annex VI); 15 July 2011.
[9] The Marine Environment Protection Committee; Resolution MEPC.304(72): Initial IMO strategy on reduction of GHG emissions from ships; 13 April 2018.
[10] United Nations Environment Programme (UNEP); Further Amendment of the Montreal Protocol: Submitted by the Contact group on HFCs. Twenty-Eighth Meeting of the Parties to the Montreal Protocol on Substances that Deplete the Ozone Layer, UNEP/OzL.Pro.28/CRP/10, Kigali, 10–14 October 2016.
[11] European Commission. Regulation (EU) No 517/2014 of the European Parliament and of the Council of 16 April 2014 on fluorinated greenhouse gases and repealing Regulation (EC) No. 842/2006, 2014.
[12] Llopis R, Sánchez D, Sanz-Kock C, Cabello R, Torrella E. Energy and environmental comparison of two-stage solutions for commercial refrigeration at low temperature: Fluids and systems. Appl Energy 2015;138:133–42.
[13] Lloyd's Naval Register, 2014. Rules and regulations for the classification of ships.
[14] DNV-GL. Rules for Classification Ships, Part 6, Additional class notations, Chapter 7. Environmental protection and pollution control. Edition January 2017.
[15] Registro Navale Italiano (RINA), 2014. Rules for the classification of ships.
[16] Bureau Veritas, 2014. Rules for the classification of steel ships.
[17] ASHRAE Standard 34 "Designation and Safety Classification of Refrigerants".
[18] Hafner A, Gabrielii CH, Widell K. Refrigeration units in marine vessels: Alternatives to HCFCs and high GWP HFCs. TemaNord: Nordic Council of Ministers; 2019.
[19] McLinden MO, Brown S, Brignoli R, Kazakov AF, Domanski PA. Limited options for low-global-warming-potential refrigerants. Nat Commun 2017;8:14476.
[20] Cao T, Lee H, Hwang Y, Radermacher R, Chun H. Performance investigation of engine waste heat powered absorption cycle cooling system for shipboard applications. Appl Therm Eng 2015;90:820–30.

[21] Lugo-Villalba RA, Guerra MA, López BS. Calculation of marine air conditioning systems based on energy savings. Ship Science & Technology 2017;11(21):103–17.
[22] Ouadha A, El-Gotni Y. Integration of an ammonia-water absorption refrigeration system with a marine Diesel engine: A thermodynamic study. Procedia Comput Sci 2013;19:754–61.
[23] Pigani L, Boscolo M, Pagan N. Marine refrigeration plants for passenger ships: Low-GWP refrigerants and strategies to reduce environmental impact. Int J Refrig 2016;64:80–92.
[24] Ahlgren F, Modejar ME, Genrup M, Thern M. Waste Heat Recovery in a Cruise Vessel in the Baltic Sea by Using an Organic Rankine Cycle: A Case Study. Journal of Engineering for Gas Turbine and Power 2016;138(1):011702.
[25] Akman M, Ergin S. An investigation of marine waste heat recovery system based on organic Rankine cycle under various engine operating conditions. Proc IMechE Part M: Journal of Engineering for the Maritime Environment 2019;233(2):586–601. https://doi.org/10.1177/1475090218770947.
[26] Salmi W, Vanttola J, Elg M, Kuosa M, Lahdelma R. Using waste heat of ship as energy source for an absorption refrigeration system. Appl Therm Eng 2016;115:501–16. https://doi.org/10.1016/j.applthermaleng.2016.12.131.
[27] Başhan V, Parlak A. Exergy analysis of the refrigerating system of a ship operating in variable sea. Journal of ETA Maritime Science 2016;4(2):149–55. https://doi.org/10.5505/jems.2016.55264.
[28] Başhan V, Parlak A. Economic analysis of a ship refrigeration system in case of variable sea water temperature conditions. Journal of ETA Maritime Science 2015;3(2):67–74. https://doi.org/10.5505/jems.2015.29392.
[29] Başhan V, Kökkülünk G. Exergoeconomic and air emission analyses for marine refrigeration with waste heat recovery system: a case study. Journal of Marine Engineering & Technology 2020;19(3):147–60. https://doi.org/10.1080/20464177.2019.1656324.
[30] Schwarz W., Rhiemeier J-M. (2007) Final report: The analysis of the emissions of fluorinated greenhouse gases from refrigeration and air conditioning equipment used in the transport sector other than road transport and options for reducing these emissions. Maritime, Rail, and Aircraft Sector. Prepared for the European Commission (DG Environment).
[31] Arpagus C, Bless F, Uhlmann M, Schiffmann J, Bertsch SS. High temperature heat pumps: Market overview, state of the art, research status, refrigerants, and application potentials. Energy 2018;152:985–1010.
[32] Arpagus C, Bless F, Schiffmann J, Bertsch SS. Multi-temperature heat pumps: A literature review. Int J Refrig 2016;69:437–65.
[33] Theotokatos G, Sfakianakis K, Vassalos D. Investigation of ship cooling system operation for improving energy efficiency. J Mech Sci Technol 2017;22(1):38–50. https://doi.org/10.1007/s00773-016-0395-9.
[34] Word sea temperature, https://www.seatemperature.org/ [Access online 07.09.2021].
[35] Aprea C, Greco A. An exergetic analysis of R22 substitution. Appl Therm Eng 2002;22:1455–69. https://doi.org/10.1016/s1359-4311(02)00066-2.
[36] Karampour M, Sawalha S. State-of-the-art integrated CO_2 refrigeration system for supermarkets: A comparative analysis. Int J Refrig 2017;86:239–57. https://doi.org/10.1016/j.ijrefrig.2017.11.006.
[37] Kim M-H, Pettersen J, Bullard CW. Fundamental process and system design issues in CO_2 vapor compression systems. Prog Energy Combust Sci 2004;30:119–74.
[38] Bruno F, Belusko M, Halawa E. CO_2 refrigeration and heat pump systems- A comprehensive review. Energies 2019;12:2959. https://doi.org/10.3390/en12152959.
[39] BITZER Kühlmaschinenbau GmbH: BITZER Software v6.15.0 rev2454; https://www.bitzer.de/ websoftware/Default.aspx?cid= [Access online 06.07.2020].
[40] Chabot A, Mathieu-Potvin F. Numerical analysis of heat pumps: selection of the best fluids for maximizing the coefficient of performance. Int J Refrig 2019;112:281–302. https://doi.org/10.1016/j.ijrefrig.2019.11.017.
[41] Llopis R, Nebot-Andrés L, Sánchez D, Catalán-Gil J, Cabello R. Subcooling methods for CO 2 refrigeration cycles: A review. Int J Refrig 2018;93:85–107. https://doi.org/10.1016/j.ijrefrig.2018.06.010.
[42] Lemmon E.W., Bell I.H., Huber M.L., McLinden M.O.: NIST Standard Reference Database 23: Reference Fluid Thermodynamic and Transport Properties-REFPROP, Version 9.1, National Institute of Standards and Technology, Standard Reference Data Program.
[43] European Parliament NEWS; https://www.europarl.europa.eu/news/en/press-room/00703IPR82633/shipping-industry-must-contribute-to-climate-neutrality-say-meps [access online 16.07.0].
[44] Kocak G, Durmusoglu Y. Energy efficiency analysis of a ship's central cooling system using variable speed pump. Journal of Marine Engineering & Technology 2018;17(1):43–51. https://doi.org/10.1080/20464177.2017.1283192.
[45] World Bunker Prices; https://shipandbunker.com/prices [access online 03.06.2021].
[46] EMBER; Daily EU ETS carbon market price (Euros); https://ember-climate.org/data/carbon-price-viewer/ [access online 18.08.2020].
[47] Markets Insider; https://markets.businessinsider.com/currencies/eur-usd [access online 18.08.2020].
[48] Government Offices of Sweden; Ministry of Finance; Presentation: Carbon Taxation in Sweden; Janurary, 2021, https://www.government.se/48e407/contentassets/419eb2cafa93423c891c09cb9914801b/210111-carbon-tax-sweden—general-info.pdf [access online 07.07.2021].
[49] Tradingeconomics; EU carbon permits; https://tradingeconomics.com/commodity/carbon [access online 11.09.2021].